Available online at www.sciencedirect.com
SCIENCE DIRECT®
International Journal of Heat and Mass Transfer 48 (2005) 5580–5601
International Journal of HEAT and MASS TRANSFER
www.elsevier.com/locate/ijhmt

Heat transfer in micro-channels: Comparison of experiments with theory and numerical results

G. Hetsroni *, A. Mosyak, E. Pogrebnyak, L.P. Yarin

Department of Mechanical Engineering, Technion—Israel Institute of Technology, Technion City, Haifa, 32000, Israel

Received 4 April 2005
Available online 25 August 2005

Abstract

This paper considers experimental and theoretical investigations on single-phase heat transfer in micro-channels. It is the second part of general exploration ''Flow and heat transfer in micro-channels''. The first part discussed several aspects of flow in micro-channels, as pressure drop, transition from laminar to turbulent flow, etc. [G. Hetsroni, A. Mosyak, E. Pogrebnyak, L.P. Yarin, Fluid flow in micro-channels, Int. J. Heat Mass Transfer 48 (2005) 1982–1998]. In this paper, the problem of heat transfer is considered in the frame of a continuum model, corresponding to small Knudsen number. The data of heat transfer in circular, triangular, rectangular, and trapezoidal micro-channels with hydraulic diameters ranging from 60 μm to 2000 μm are analyzed. The effects of geometry, axial heat flux due to thermal conduction through the working fluid and channel walls, as well as the energy dissipation are discussed. We focus on comparing experimental data, obtained by number of investigators, to conventional theory on heat transfer. The analysis was performed on possible sources of unexpected effects reported in some experimental investigations.

Keywords: Micro-channel; Laminar flow; Heat transfer; Energy dissipation; Axial conduction

1. Introduction

Heat transfer in straight tubes and channels was the subject of numerous researches for the last century. The predictions of this theory agree fairly well with known experimental data related to heat transfer in the conventional size straight channels [1–4]. The development of micro-mechanics, stimulated during the last decades, a great interest to study flow and heat transfer in micro-channels [5,6]. A number of theoretical and experimental investigations devoted to this problem were performed during 1995–2005 [7–23]. The data on heat transfer in laminar and turbulent flows in micro-channels with different geometry were obtained. Several special problems related to heat transfer in micro-channels were discussed: effect of axial conduction in the wall and viscous dissipation effect [24–29]. Comprehensive surveys may be found in [30–37].

Comparison between experimental correlations for the Nusselt number in micro-channels, for gas and liquid flow, is shown in Fig. 1a and b. Considering available

* Corresponding author. Tel.: +972 4 829 2058; fax: +972 4 823 8101.
E-mail address: hetsroni@techunix.technion.ac.il (G. Hetsroni).

0017-9310/$ - see front matter © 2005 Elsevier Ltd. All rights reserved.
doi:10.1016/j.ijheatmasstransfer.2005.05.041

Nomenclature

Br	Brinkman number
c_p	specific heat
d, D_{in}	inner diameter of micro-tube
D_h	hydraulic diameter of micro-channel
F_{cond}	conductive heat flux
F_{conv}	convective heat flux
H	micro-channel height
Kn	Knudsen number
k_s, k	average height of roughness
L	micro-channel length
L_h	heating length
L_d	length of development section
$\overline{L}$	dimensionless length of micro-channel
M	conductive to convective heat flux ratio
Nu	Nusselt number
Nu_{av}	average Nusselt number
Nu_{th}	theoretical value of Nusselt number
Pe	Peclet number
Pr	Prandtl number
q	heat flux
Re	Reynolds number
r_0	micro-tube radius
R	dimensionless distance from micro-tube axis
r	radial coordinate
T	temperature
$\overline{T}$	average temperature
u	velocity
$\bar{u}$	average velocity
x	longitudinal coordinate
X	dimensionless longitudinal coordinate

Greek symbols

δ	thickness of micro-tube
λ	thermal conductivity
μ	dynamic viscosity
ν	kinematic viscosity
θ	dimensionless temperature
ρ	density

Subscripts

1	fluid
2	wall
av	average
th	theoretical
in	inlet
2.1	ratio parameter of wall to fluid

results about experimental researches on heat transfer, one can conclude that there is a large scatter in the results. There are not convincing explanation of the difference between experimental and theoretical results, obtained in laminar flow and between experimental and semi-empirical results obtained in turbulent flow. On the one hand, it can be interpreted as displaying some new effects of heat transfer in flow in micro-channels [5,25–27,38]. On the other hand, the phenomenon may be related to the discrepancy between the actual conditions of a given experiment, and theoretical or numerical solution obtained in the frame of conventional theory [39,40]. The aim of the present study is to address this issue.

For analysis we discuss experimental results of heat transfer obtained by previous investigators and related to laminar, incompressible, fluid flow in micro-channels of different geometry: circular tubes, rectangular, trapezoidal and triangular channels. The basic characteristics of experimental conditions are given in Table 1. The studies considered in the present paper were selected to reveal the physical basis of scale effect on convective heat transfer and mainly confined to consideration of laminar flows that are important for comparison with conventional theory.

2. Experimental investigations

2.1. Heat transfer in circular tubes

2.1.1. Laminar flow

The schemes of the test sections are shown in Fig. 2. The geometrical parameters are presented in Tables 2 and 3. Fig. 2a shows the experimental setup used by Lelea et al. [23]. The inner diameters of smooth micro-tubes were 125.4, 300, and 500 μm and the flow regime was laminar with Reynolds number $Re = 95$–774. The micro-tube was placed inside a vacuum chamber to eliminate heat loss to the ambient. It was heated by Joule heating with an electrical power supply. Distilled water was used and the measurements of heat transfer coefficient were performed under thermal boundary condition of constant heat flux on the wall. In the experimental setup, there were two electrodes at both ends of the test tube. The insulated parts were included in the test section. So that, for heating length of $L_h = 250$, 95, and 53 mm the total length of the test sections was $L = 600$, 123, and 70 mm, respectively. The experimental results have been compared both with theoretical predictions from the literature, and the results obtained by numerical modeling under the same thermal boundary

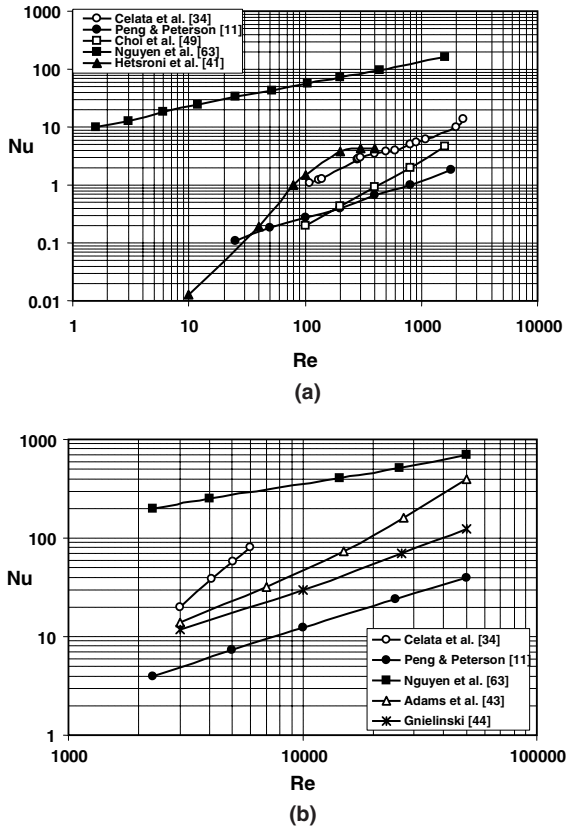

Fig. 1. Comparison between the experimental correlations for the Nusselt number in micro-channels. (a) Laminar flow and (b) turbulent flow.

conditions at the inlet and outlet of the tube. The experimental results confirm that, including the entrance effects, the conventional theories are applicable for water flow through micro-channels, Fig. 3a.

The micro-channels utilized in engineering are frequently connected with inlet and outlet manifolds. In this case the thermal boundary condition at the inlet and outlet of the tube is not adiabatic. Heat transfer in micro-tube under these conditions was studied by Hetsroni et al. [41]. They measured heat transfer of water flowing in a pipe of inner diameter 1.07 mm, outer diameter 1.5 mm, and 0.600 m in length, Fig. 2b. It was divided into two sections. The development section of length $L_d = 0.245$ m was used for the flow and the thermal field development. The test section of heating length $L_h = 0.335$ m was used for collecting the experimental data. DC current was supplied through the development and test sections for direct heating. The outer temperature on the heated wall was measured by means of infrared radiometer. Experiments were carried out in the range of Reynolds number $Re = 10$–450. The average Nusselt number was calculated using the average temperature of the inner tube wall and mean temperature of the fluid at the inlet and outlet of the tube.

The dependence of the average Nusselt number on the Reynolds number is presented in Fig. 3b. The Nusselt number increased drastically with increasing Re at very low Reynolds numbers, $10 < Re < 100$, but this increase became smaller for $100 < Re < 450$. Such a behavior was attributed to effect of axial heat conduction through the tube wall. Fig. 3c shows the dependence of the relation N_a/N on the Peclet number, Pe, where N_a is the power conducted axially through the tube wall, N is total electrical power supplied to the tube. Comparison between the results presented in Fig. 3b and those presented in Fig. 3c allows one to conclude that the effect of thermal conduction through the solid wall leads to a decrease in the Nusselt number. This effect decreases with an increase in the Reynolds number. It should be stressed that the heat transfer coefficient depends on the character of the wall temperature and the bulk fluid temperature variation along the heated tube wall. It is well known that under certain conditions the use of mean wall and fluid temperature to calculate the heat transfer coefficient may lead to peculiar behavior of the Nusselt number [1,2,42]. The experimental results of Hetsroni et al. [41] showed that the use of heat transfer model based on the assumption of constant heat flux, and linear variation of the bulk temperature of the fluid at low Reynolds number, yield an apparent growth of the Nusselt number with increase in the Reynolds number, as well as underestimation of this number.

Table 1
Basic characteristics of micro-channels and experimental conditions

Geometry of micro-channels	Micro-channels sizes			Working fluid	Walls		Re
	D_h [μm]	L_h [mm]	L/D_h		Material	Surface	
Circular	125.4–1070	53–335	72–500	Distilled water de-ionized water	Stainless steel	Smooth rough	10–2600
Rectangular	133–2000	25–325.125	13–433	De-mineralized water, de-ionized water	Silicon, copper	Smooth rough	40–9000
Trapezoidal and triangular	62.3–168.9	30	180–500	R 134a FC-84	Silicon	Smooth rough	15–1450

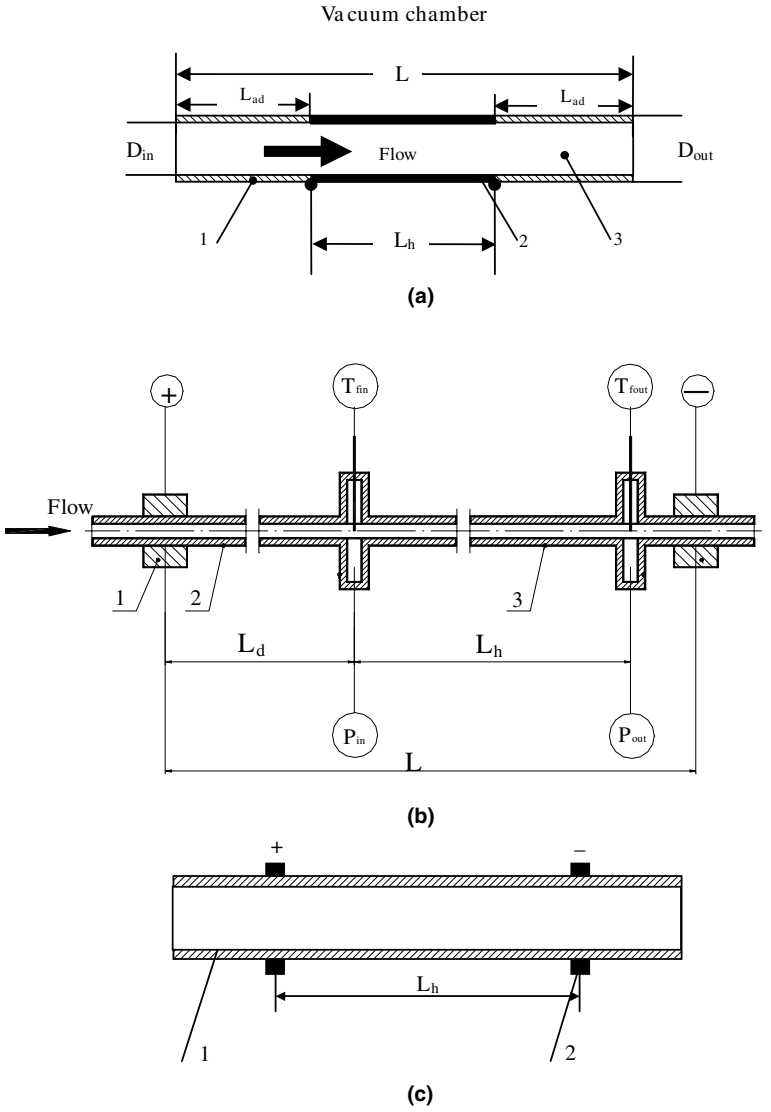

Fig. 2. Circular micro-channels (a) $D_{in} = 125.4$–500 μm. Test section used by Lelea et al. [23]; 1—Adiabatic section, 2—heated section, 3—micro-channel, (b) $D_{in} = 1070$ μm. Test section used by Hetsroni et al. [41]; 1—Electrical contact, 2—thermal developing section, 3—measurement section, (c) test section of rough circular micro-channel used by Kandlikar et al. [50]. $D_{in} = 1067$ μm, $k/D_{in} = 0.00178$–0.00281; $D_{in} = 620$ μm, $k/D_{in} = 0.00161$–0.00355; 1—steel tube, 2—electrical contact.

Table 2
Smooth circular micro-channels and experimental conditions

Author	Number of channels in the test section, n	Inner diameter, D_{in} (μm)	Outer diameter, D_{out} (μm)	Heating length, L_h (mm)	Dimensional length, L_h/D_{in}	Reynolds number, Re
Lelea et al. [23]	1	500	700	250	500	
		300	500	95	317	95–774
		125.4	300	53	424	
Hetsroni et al. [41]	1	1070	1500	335	313	10–450

Table 3
Rough circular micro-channels and experimental conditions

Author	Number of channels in the test section, n	Inner diameter, D_{in} (μm)	Relative roughness, k/D_{in}	Heating length, L_h (mm)	Dimensional length, L_h/D_{in}	Reynolds number, Re
Kandlikar et al. [50]	1	1067	0.00178–0.00281	76.5	72	500–2600
		620	0.00161–0.00355	67	108	

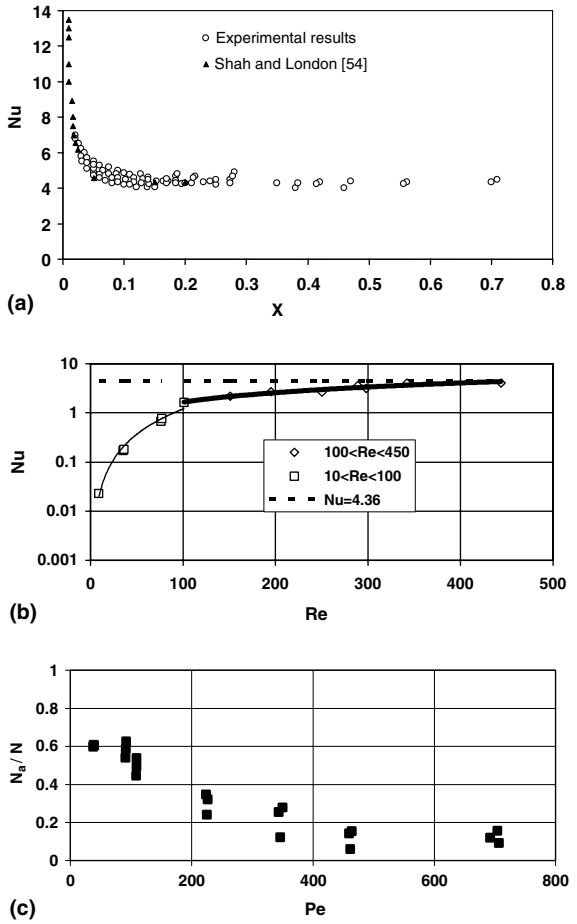

Fig. 3. Experimental results for smooth circular tubes: (a) dependence of the Nusselt number on non-dimensional axial distance $D_{in} = 125.4$, 300 and 500 μm, $Re = 95$–774 [23], (b) D_{in} 1070 μm. Dependence of average Nusselt number on Reynolds number [41], (c) $D_{in} = 1070$ μm. Dependence of the relation of the power conducted axially through the heated wall to the power supplied to the heat section [41].

2.1.2. Turbulent flow

Adams et al. [43] investigated turbulent, single phase forced convection of water in circular micro-channels with diameters of 0.76 and 1.09 mm. The Nusselt numbers determined experimentally were higher than would be predicted by traditional Nusselt number correlations such as the Gnielinski correlation [44]. The data suggest that the extent of enhancement (deviation) increases as that channel diameter decreases. Owhaib and Palm [45] investigated the heat transfer characteristics for single phase forced convection of R 134 through single circular micro-channels. The test sections consisted of stainless steel tubes with 1.7, 1.2, and 0.8 mm inner diameters, and 325 mm in length. The results show good agreement between the classical correlations [46,47,44] and the experimentally measured data in the turbulent region. Contrary, correlations suggested for micro-channels [48,49,43] do not agree with this test. Kandlikar et al. [50] studied experimentally the effect of surface roughness on the heat transfer in circular tubes of diameter 1.067 mm and 0.62 mm. Brief characteristics of these experiments are given in Fig. 2c and Table 3. The results are presented in Fig. 4a and b. The authors

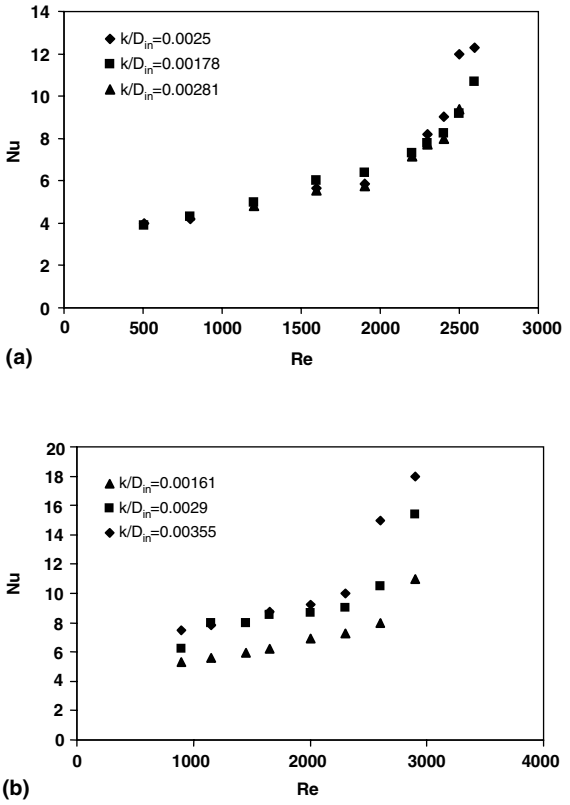

Fig. 4. Plots of local Nusselt number for different k/D_{in} ratios [50]. (a) $D_{in} = 1067$ μm, (b) $D_{in} = 620$ μm.

concluded that tubes above $D_{in} = 1.067$ mm with relative roughness k/D_i about 0.003 may be considered as smooth tubes. However, for small diameter tubes ($D_{in} < 0.62$ mm), the same relative roughness value increases the heat transfer.

2.2. Heat transfer in rectangular, trapezoidal and triangular ducts

The schemes of the test sections are shown in Fig. 5. The geometrical parameters are presented in Tables 4 and 5. Peng and Peterson [11] investigated experimentally the single-phase forced convective heat transfer of water in micro-channel structures with small rectangular channels having hydraulic diameter of 0.133–0.367 mm and distinct geometric configuration, Table 4, Fig. 5a. The heat flux of the micro-channel structure was based on the micro-channel plate area. The heat transfer coefficient was evaluated using log-mean temperature difference. Thus, the heat transfer coefficient corresponds to some integral value of heat flux. The dependence of the heat transfer coefficient on the flow and the geometric parameters was presented.

Harms et al. [51] obtained experimental results for single-phase forced convection in deep rectangular micro-channels, Table 4, Fig. 5b. Two configurations were tested, a single channel system and a multiple channel system. All tests were performed with deionized water, the Reynolds number ranged from 173 to 12,900. For the single channel design, the experimental Nusselt number was higher than theoretically predicted for heat transfer in laminar flow. For example, at $Re = 1383$ the Nusselt number was $Nu = 40.9$. The authors conclude this enhancement may be due to the effect of the inlet bend. The results for the multiple channel design in the range $Re = 173$–1188 showed an increase in Nusselt number with increasing Re. For example, at $Re = 173$ the Nusselt number was $Nu = 2.65$, and at $Re = 1188$ the Nusselt number was $Nu = 8.41$. This deviation from theoretical prediction was attributed, by the authors, to flow bypass in the manifold. The authors believe that in systems with a small heater area compared to the projected channel area, three-dimensional conduction occurs. However, for multiple channel design three-dimensional conduction also occurs when the heater area covers the entire projected channel area.

Qu and Mudawar [52] studied both experimentally and numerically heat transfer characteristics of a single phase micro-channel heat sink. The heat sink was fabricated of oxide-free copper and fitted with a polycarbonate plastic cover plate, Fig. 5c. The heat sink consisted of an array of rectangular micro-channels 231 μm wide and 713 μm deep, Table 4. The Reynolds number ranged from 139 to 1672. The three-dimensional heat transfer characteristics of the heat sink were analyzed numerically by solving the conjugate heat transfer problem. The measured temperature distributions showed good agreement with the corresponding numerical predictions, Fig. 6a. These findings demonstrate that conventional Navier–Stokes and energy equations can adequately predict the fluid flow and heat transfer characteristics of micro-channel heat sinks.

Warier et al. [53] conducted experiments of forced convection in small rectangular channels using FC-84 as the test fluid. The test section consisted of five parallel channels with hydraulic diameter of $D_h = 0.75$ mm and length to diameter ratio $L_h/D_h = 433.5$, Fig. 5d, Table 4. The experiments were performed with uniform heat fluxes applied at the top and bottom surfaces. The wall heat flux was calculated using the total surface area of the flow channels. Variation of single-phase Nusselt number with axial distance is shown in Fig. 6b. The numerical results presented by Kays and Crawford [2] are also shown in Fig. 6b. The measured values agree quite well with the numerical results.

The study of Gao et al. [18] is devoted to investigations of the flow and the associated heat transfer in micro-channels of large-span rectangular cross-section and adjustable height in the range of 0.1–1 mm, Fig. 5e, Table 4. The fluid used was demineralized water. The active channel walls were two plane brass blocks of heating length $L = 62$ mm, which were separated by a foil with a hollowed out central part of width $b = 25$ mm. The thickness of this foil fixed the channel height, H. A set of foils allowed variations of the hydraulic diameter $D_h = 200$–2000 μm. A typical temperature distribution along the channel for the case of a very narrow micro-channel ($D_h = 200$ μm) is shown in Fig. 6c. The local Nusselt number, $Nu(x)$, expressed as a function of $X = x/(D_h Pe)$ was compared with the theoretical solution of Shah and London [54]. For $D = 1000$ μm the results demonstrate good agreement with theoretical solution. However, for $H = 100$ μm, the plot $Nu(X)$ shows departure from theoretical heat transfer law, the Nusselt number is smaller than the conventional value for large-scale channels. This trend is in agreement with results reported by Qu et al. [16]. Fig. 6d shows the dependence of Nu_{av}/Nu_{th} as a function of the channel height, where Nu_{th} is the theoretical value of the Nusselt number for the same value of X. The significant reduction in the Nusselt number cannot be explained by roughness effects. The modification of heat transfer laws by electro kinetic effects also are to be discarded, due to the large difference of scales between the channel height and the double diffusive layer thickness.

An experimental investigation was conducted by Lee et al. [55] to explore the validity of classical correlations based on conventional-sized channels for predicting the thermal behavior in single-phase flow through rectangular micro-channels. The micro-channels ranged in width from 194 μm to 534 μm, with the channel depth being nominally five times the width in each case, Fig. 5f,

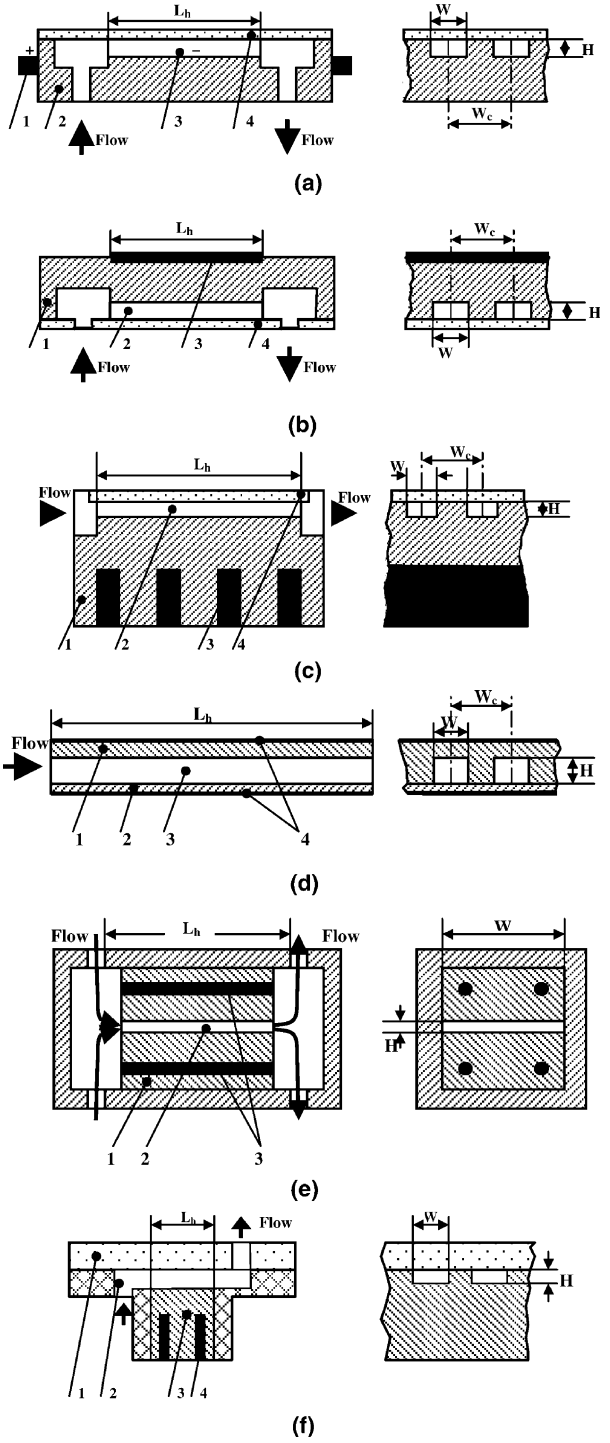

Fig. 5. Rectangular micro-channels: (a) $D_h = 133$–367 μm. Test section used by Peng and Peterson [11]: 1—Electrical contact, 2—heated stainless steel block, 3—micro-channel, 4—cover plate. (b) $D_h = 404$–1923 μm. Test section used by Harms et al. [51]: 1—Silicon wafer, 2—micro-channel, 3—heater, 4—cover plate. (c) $D_h = 348$ μm. Test section used by Qu and Mudawar [52]: 1—Copper block, 2—micro-channel, 3—heater, 4—cover plate. (d) $D_h = 750$ μm. Test section used by Warrier et al. [53]: 1—Upper aluminum plate, 2—down aluminum plate, 3—micro-channel, 4—heater. (e) $D_h = 200$–2000 μm. Test section used by Gao et al. [18]: 1—Brass block, 2—micro-channel, 3—heater. (f) Thermally developing flow in rectangular micro-channel, Lee et al. [55]: 1—Cover plate, 2—micro-channel, 3—copper block, 4—heater.

Table 4
Rectangular micro-channels

Author	Number of channels in the test section, n	Width, W (μm)	Height, H (μm)	Distance between channels, W_c (μm)	Heating length, L_h (mm)	Hydraulic diameter, D_h (μm)	Dimensional length, L_h/D_h	Reynolds number, Re
Peng and Peterson [11]	Not reported	100–400	200–300	2000 4500	45	133–367	123–338	90–9000
Harms et al. [51]	1	25,000	1000	–	25	1923	13	173–12,900
	68	251	1030	370		404	62	
Qu and Mudawar [52]	21	231	713	467	44.764	348	129	139–1672
Warrier et al. [53]	5				325.125	750	433.5	557–1552
Gao et al. [18]	1	25,000	100–1000		62	200–2000	31–310	40–8000
Lee et al. [55]	10	194–534	884–2910		25.4	318–903	28–80	300–3500

Table 4. Each test piece was made of copper and contained ten micro-channels in parallel. The experiments were conducted with deionized water, with the Reynolds number ranging from approximately 300 to 3500. The tests were carried out either at hydrodynamically developed but thermally developing (TD) or a simultaneously developing (SD) regime. The average heat transfer coefficient was determined by using the area available for convection of channels, average temperature of the channel wall and mean fluid temperature at the inlet and outlet of the micro-channels. In Fig. 6e, the numerical calculations that did not include the conduction in the substrate are compared with experimental results.

Qu et al. [16] carried out experiments on heat transfer for water flow at $100 < Re < 1450$ in trapezoidal silicon micro-channels, with a hydraulic diameter ranging from 62.3 to 168.9 μm. The dimensions are presented in Table 5 where W_t and W_b is the upper and lower basis of the trapezoidal channel, H is the height of the channel. A numerical analysis was also carried out by solving a conjugate heat transfer problem involving simultaneous determination of the temperature field in both the solid and fluid regions. It was found that experimentally determined Nusselt number in micro-channels is lower than that predicted by numerical analysis. A roughness-viscosity model was applied to interpret the experimental results.

Wu and Cheng [20] investigated laminar convective heat transfer of water in a single trapezoidal silicon micro-channel. They used a set of 13 micro-channels having different dimensions and different relative roughness. The geometrical parameters of micro-channels are presented in Table 5. The silicon chip was anodically bonded with a thin Pyrex glass plate from the top. Fig. 7a shows the effect of surface roughness on the Nusselt number. One can see that at the same Reynolds numbers the Nusselt number increases with increasing relative surface roughness. The laminar convective heat transfer showed two different characteristics at low and high Reynolds number ranges. Fig. 7b shows effect of geometric parameters on the Nusselt number. From Fig. 7b, it can be observed that for very low Reynolds number flow, $Re = 0$–100, the Nusselt number increased acutely with the increase in the Reynolds number. However, the increase in the Nusselt number after $Re = 100$ is gentle with the increase in the Reynolds number.

3. Effect of viscous energy dissipation

Under some conditions, the heat released due to viscous dissipation leads to drastic change of flow and temperature field, in particular, it leads to flow instability, transition to turbulence hydrodynamic thermal explosion, oscillatory motions, etc. [56–58]. This problem was also discussed by Tso and Mahulikar [25–27]. To reveal the effect of viscous dissipation, the experimental data by Wang and Peng [9] and Tso and Mahulikar [27] were used. Experiments were performed using water flow in micro-channel specimens, the experimental data in laminar flow regime were found to correlate well with the Brinkman number. As a result, a semi-empirical equation for the Nusselt number was suggested and the dependence of $Nu/Re^{0.62}Pr^{0.33}$ on the Brinkman number, Br, was demonstrated. However, most of the data used for the correlation with Br were obtained under conditions, in which the Reynolds number and the Prandtl number also varied, so that it was difficult to distinguish the effect of the Brinkman number from effects of the Reynolds number and the Prandtl number. So, at $0.4559 \times 10^{-5} \leqslant Br \leqslant 2.8333 \times 10^{-5}$ the Reynolds number and the Prandtl number change in the ranges of $80 \leqslant Re \leqslant 107$, $4.80 \leqslant Pr \leqslant 6.71$ (Table 1 presented by Tso and Mahulikar [25]). To estimate the real effect of viscous dissipation on heat transfer it is necessary to determine the dependence of the Nusselt number on the Brinkman number at fixed values of the Reynolds and the Prandtl numbers. Such a presentation of the data reported by Tso and Mahulikar [25] is shown in Table 6. It is seen that the effect of the Brinkman number

Table 5
Trapezoidal and triangular micro-channels

Author	Number of channels in the test section, n	Width (top), W_t (μm)	Width (bottom), W_b (μm)	Height, H (μm)	Length, L (mm)	Hydraulic diameter, D_h (μm)	Dimensional length, L/D_h	Relative roughness k/D_h	Reynolds number, Re
Qu et al. [16]	5	198.33	94.83	35.41	30	62.3	482	1.118E−2	100–1450
		523.20	356.32	111.14		168.9	178	1.75E−2	
Wu and Cheng [20]	13	157.99–1473	0–1375	56.22–110.7			195.34–453.79	3.26E−5–1.09E−2	15–1500
Tiselj et al. [59]	17	310	0		10	160	63		3.2–84

on the Nusselt number is negligible. The same conclusion may be derived also from experiments performed by Tso and Mahulikar [27]. According to their measurements, Table 7, the variation of the Brinkman number from 1.1195×10^{-8} to 2.3048×10^{-8} did not affect the Nusselt number, when the Reynolds and the Prandtl numbers did not change significantly. It should be stressed that the effect of the viscous dissipation on heat transfer in micro-channels at extremely small values of the Brinkman numbers ($Br \sim 10^{-8}$–10^{-5}) is non-realistic from the physical point of view. The Brinkman number, $Br = \mu U^2/\lambda \Delta T$, is the ratio of the heat production due to viscous forces, to heat transferred from the wall to the fluid. At small Br the contribution of the heat released due to viscous forces is negligible, consequently the effect on the heat transfer is also negligible. It should be also noted that evaluation of the role of the Brinkman number performed by Tso and Mahulikar [25–27] was based on the experiments that were carried out under some specific conditions (the heat transfer characteristics were found to be affected by the channel geometry, axial heat conduction through the channels walls, liquid velocity and temperature, etc.). Some aspects of this problem were discussed by Herwig and Hausner [40] and Gad-el-Hak [38].

The effect of viscous heating was investigated by Tunc and Bayazitoglu [28] when the fluid was heated ($T_{in} < T_w$) or cooled ($T_{in} > T_w$). In the range of the Knudsen numbers $0 < Kn < 0.12$ the Nusselt number decreased as the Knudsen number increased. The viscous dissipation significantly affected heat transfer. The authors showed that the decrease was greater when viscous dissipation occurred. The effect of viscous dissipation on the temperature field was investigated by Koo and Kleinstreuer [29] for three working fluids: water, methanol and iso-propanol. Channel size, the Reynolds number and the Prandtl number are the key factors which determine the impact of viscous dissipation. Viscous dissipation effects may be very important for fluids with low specific heats and high viscosities, even in relatively low Reynolds number flows. For water the relative magnitude of the ratio, A, of convective heat transfer to dissipation term is given in Table 8.

Experimental and numerical analysis were performed on the heat transfer characteristics of water flowing through triangular silicon micro-channels with hydraulic diameter of 160 μm in the range of Reynolds number $Re = 3.2$–84 [59]. It was shown that dissipation effects can be neglected and the heat transfer may be described by conventional Navier–Stokes and energy equations as a common basis. Experiments carried out by Hetsroni et al. [41] in a pipe of inner diameter of 1.07 mm also did not show effect of the Brinkman number on the Nusselt number in the range $Re = 10$–100.

Hetsroni et al. [60] evaluated the effect of inlet temperature, channel size and fluid properties on energy

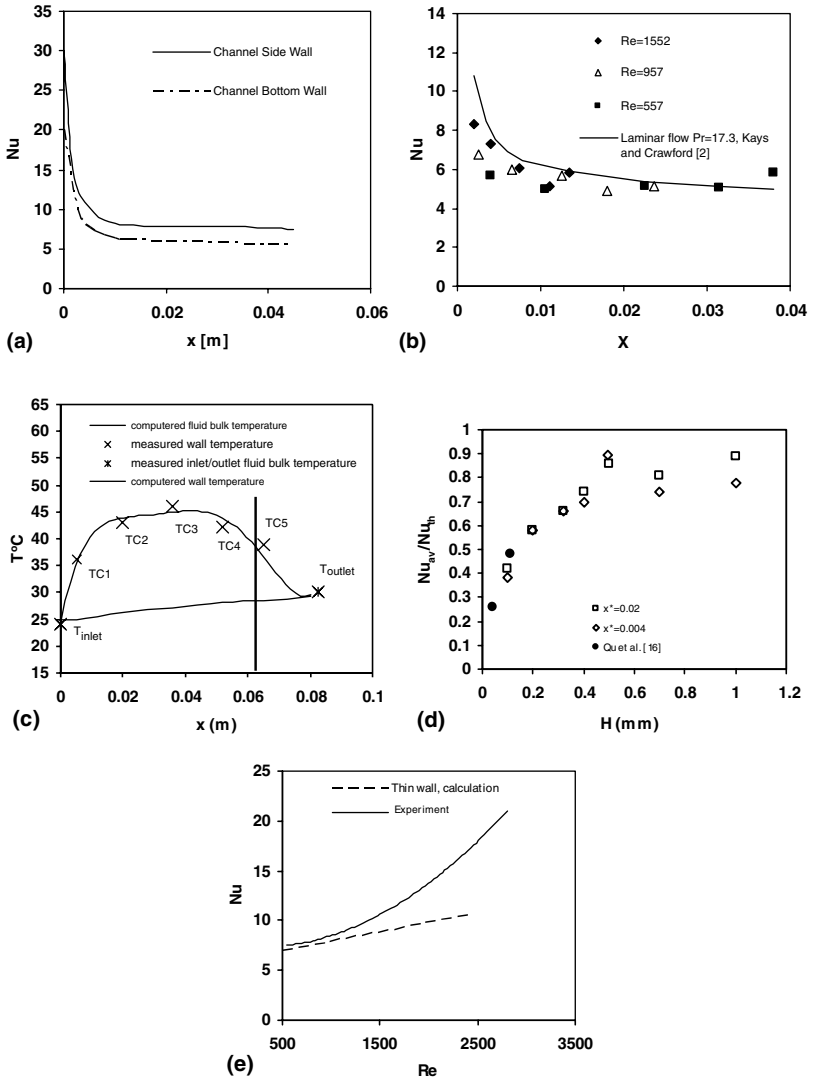

Fig. 6. Rectangular micro-channels. Calculation and experimental data (a) $D_h = 348$ μm. Numerical predictions of average Nusselt number, $Re = 864$ [52], (b) $D_h = 750$ μm. Variation of Nusselt number with axial distance, Warrier et al. [53], (c) $D_h = 200$ μm, $Re = 1780$. Temperature distribution along the channel Gao et al. [18], (d) $D_h = 200$–2000 μm. Effect of channel size on Nusselt number, Gao et al. [18], (e) Comparison of the average Nusselt number obtained from numerical analyses for the 194 μm wide micro-channels, Lee et al. [55].

dissipation in the flow of viscous fluid. For fully developed laminar flow in circular micro-channels, they obtained an equation for the adiabatic increase of the fluid temperature due to viscous dissipation:

$$\frac{\Delta T}{T_{in}} = 2\frac{v^2}{r_0^2}\left(\frac{L}{r_0}\right)\frac{Re}{c_p T_{in}} \quad (1)$$

For an incompressible fluid, the density variation with temperature is negligible compared to the viscosity variation. Hence, the viscosity variation is a function of temperature only and can be a cause of radical transformation of flow and transition from stable flow to oscillatory regime. The critical Reynolds number depends significantly also on the specific heat, Prandtl number and micro-channel radius. For flow of high viscous fluids in micro-channels of $r_0 < 10^{-5}$ m the critical Reynolds umber is less than 2300. In this case the oscillatory regime occurs at values of Reynolds number $Re < 2300$.

We estimate the values of the Brinkman number, at which the viscous dissipation becomes important: assuming that the physical properties of the fluid are constant, the energy equation for fully developed flow in circular tube at $T_w = \text{const}$ is

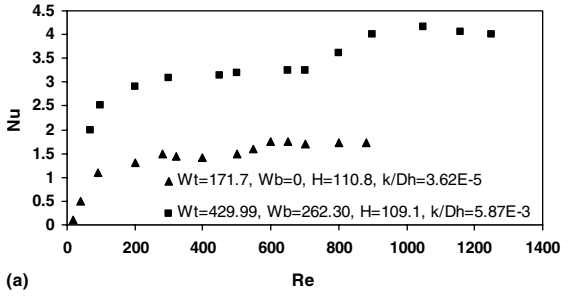

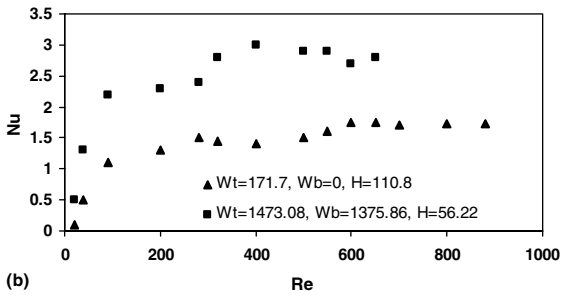

Fig. 7. Trapezoidal micro-channels. (a) Effect of surface roughness on Nusselt number, Wu and Cheng [20]. (b) Effect of geometric parameters on Nusselt number, Wu and Cheng [20].

Table 6
Experimental data in the laminar regime presented by Tso and Mahulikar [25] at approximately fixed values of the Reynolds and the Prandtl numbers

$Br\times10^5$	Re	Pr	Nu
0.4559	107	4.80	0.35
1.4541	124	4.82	0.37
2.8333	80	6.71	0.46
4.4115	93	6.62	0.49

Table 7
Experimental data in the laminar regime obtained by Tso and Mahulikar [27] at approximately fixed values of the Reynolds and the Prandtl numbers

$Br\times10^8$	Re	Pr	Nu
1.1195	17.5	3.50	0.3031
2.3048	22.4	3.82	0.3068

Table 8
Ratio, A, of convective heat transfer to dissipation term in tubes

Tube radius R_0, m	$Re=20A$	$Re=200A$	$Re=2000A$
10^{-3}	3.45×10^4	3.45×10^3	3.45×10^2
10^{-4}	3.45×10^2	3.45×10^1	3.45×10^0
10^{-5}	3.45×10^0	3.45×10^{-1}	3.45×10^{-2}

$$\rho u c_p \frac{\partial T}{\partial x} = \frac{1}{r}\frac{\partial}{\partial r}\left(\lambda r \frac{\partial T}{\partial r}\right) + \mu\left(\frac{\partial u}{\partial r}\right)^2 \tag{2}$$

where ρ, μ and λ are the density, viscosity and thermal conductivity, respectively, and c_p is the specific heat, u is the actual velocity.

The actual velocity, u, may be expressed as

$$u = 2\bar{u}(1-R^2) \tag{3}$$

where $\bar{u} = \frac{1}{r_0^2}\int_0^{r_0} ur\,\mathrm{d}r$ is the average velocity, $R = \frac{r}{r_0}$, r_0 is the micro-channel radius.

Rewriting Eq. (2) in divergent form and integrating it we obtain:

$$\frac{2\int_0^{r_0}\frac{\partial}{\partial x}\{\rho u c_p(T-T_w)\}r\,\mathrm{d}r}{\lambda(\overline{T}-T_w)} = -Nu \pm 8Br \tag{4}$$

where $\overline{T}$ is the average fluid temperature, T_w is the wall temperature, $Nu = -\frac{\lambda(\frac{\partial T}{\partial r})_{r=r_0}d}{\lambda(\overline{T}-T_w)}$ is the Nusselt number, $Br = \frac{\mu u^2}{\lambda|\overline{T}-T_w|}$ is the Brinkman number. The minus or plus sign in front of the last term in Eq. (4) corresponds to cooling of fluid when $\overline{T}_0 > T_w$ or its heating $\overline{T}_0 < T_w$, respectively, $\overline{T}_0$ is the average fluid temperature at the inlet of the micro-channel.

To estimate the value of the term in the left hand side of Eq. (4) we use an approximate expression for the local and average fluid temperature in the tube. We use as the first approach the expressions of $T(x,r)$ and $\overline{T}(x)$ that correspond to negligible viscous dissipation. For $T_w = \text{const}$ they are:

$$T - T_w = (T_0 - T_w)\sum_{n=0}^{\infty} A_n\varphi_n(R)\exp\left(-2\varepsilon_n^2\frac{1}{Pe}\frac{x}{d}\right) \tag{5}$$

$$\overline{T} - T_w = 8(\overline{T}_0 - T_w)\sum_{n=1}^{\infty}\frac{B_n}{\varepsilon_n^2}\exp\left(-2\varepsilon_n^2\frac{1}{Pe}\frac{x}{d}\right) \tag{6}$$

where $Pe = \bar{u}d/\alpha$ is the Peclet number, α is the thermal diffusivity, ε_n and A_n, B_n are the known eigenfunctions and constants [1].

For large values of dimensionless axial distance, $X = \frac{1}{Pe}\frac{x}{d}$ the following relations were obtained from Eqs. (4)–(6):

$$T - T_w = (T_0 - T_w)A_0\varphi_0(R)\exp\left(-2\varepsilon_0^2\frac{1}{Pe}\frac{x}{d}\right) \tag{7}$$

$$\overline{T} - T_w = 8(\overline{T}_0 - T_w)\frac{B_0}{\varepsilon_0^2}\exp\left(-2\varepsilon_0^2\frac{1}{Pe}\frac{x}{d}\right) \tag{8}$$

and

$$-2\frac{\frac{\mathrm{d}}{\mathrm{d}x}\int_0^{r_0}\rho u c_p Tr\,\mathrm{d}r}{\lambda(\overline{T}-T_w)} = \frac{1}{4}\varepsilon_0^4\frac{A_0}{B_0}\int_0^1(1-R^2)\varphi_0(R)R\,\mathrm{d}R \tag{9}$$

Substitution of the values of $\varepsilon_0 A_0$, B_0, as well as the expression for $\varphi_0(R)$ in the right hand side of Eq. (9) gives:

$$\frac{1}{4}\varepsilon_0^4\frac{A_0}{B_0}\int_0^1(1-R^2)\varphi_0(R)R\,\mathrm{d}R = 3.64 = Nu_0 \tag{10}$$

where Nu_0 is the Nusselt number that corresponds to negligible viscous dissipation.

Eq. (4) is rewritten as

$$Nu = Nu_0 \pm 8Br \tag{11}$$

where sign plus and minus correspond to the cooling $\overline{T}_0 > T_w$ or heating $\overline{T}_0 < T_w$ regimes, respectively.

Eq. (11) indicates the effect of viscous dissipation on heat transfer in micro-channels. In the case when the inlet fluid temperature, T_0, exceeds the wall temperature viscous dissipation leads to an increase in the Nusselt number. In contrast to that, when $\overline{T}_0 < T_w$, viscous dissipation leads to a decrease in the temperature gradient on the wall. Eq. (11) corresponds to relatively small amount of heat released due to viscous dissipation. Taking this into account, we estimate the lower boundary of the Brinkman number at which the effect of viscous dissipation may be observed experimentally. Assuming that $\frac{Nu-Nu_0}{Nu_0} \geqslant 10^{-2}$ the following evaluation of the Brinkman number was obtained: $Br \geqslant 5 \cdot 10^{-3}$. This estimation shows that the conclusions of Tso and Mahulicar [25–27] cannot be derived from experiments performed at extremely low Brinkman numbers ($Br \sim 10^{-8}$–10^{-5}).

It should be emphasized that under conditions of energy dissipation the definition of the heat transfer coefficient as $\lambda\left(\frac{\partial T}{\partial r}\right)_{r=r_0}/(\overline{T} - T_w)$, where T is the fluid temperature, T_w is the wall temperature, does not characterize the intensity of the heat transferred [2,4].

There are two factors that determine the temperature distribution of the fluid: (i) convective heat transfer, (ii) heat released due to viscous dissipation. For cooling regime when the fluid temperature at the inlet $T_0 > T_w$ convective heat transfer from the fluid to the wall leads to a decrease in the fluid temperature along relatively small dimensionless distance X. The heat released due to viscous dissipation causes an increase in the fluid temperature. The contribution of each component to the behavior of the fluid temperature depends on X. At small X the dominant role plays convective heat transfer whereas at large X, the effect of viscous dissipation becomes significant. Superposition of these two factors determines the specific shape of the temperature distribution along the micro-channel: the fluid temperature variation along micro-channel has a minimum. Noteworthy, that under condition of viscous dissipation the fluid temperature does not reach the wall temperature at any value of X.

For heating regime at small X, the heat from the wall to the cold fluid and the heat released due to viscous dissipation lead to increase in fluid temperature. At some value of X the fluid temperature may exceed the wall temperature, Fig. 8a. The difference $T - T_w$ decreases up to the inversion point $X = X_{inv}$. That leads to physically unrealistic results as infinite growth of the Nusselt number in the vicinity of the inversion point. The analysis of the behavior of the fluid temperature and the Nusselt number performed for circular tube at thermal wall boundary condition $T_w = \text{const}$ reflects also general features of heat transfer in micro-channels of other geometry.

4. Axial conduction

4.1. Axial conduction in the fluid

This problem was the subject of a number of theoretical investigations carried out for conventional size channels [1,21,61–63]. We consider the effect of axial conduction in the fluid on heat transfer in micro-channels. The energy equation was used for the flow of incompressible fluid with constant physical properties. Assuming that the energy dissipation is negligible:

$$\rho u c_p \frac{\partial T}{\partial x} = \lambda\left\{\frac{1}{r}\frac{\partial}{\partial r}\left(r\frac{\partial T}{\partial r}\right) + \frac{\partial^2 T}{\partial x^2}\right\} \tag{12}$$

where x and r are the longitudinal and radial coordinates, ρ, c_p and λ are the density, specific heat and thermal conductivity of the fluid, respectively.

For $q = \text{const}$ (q is the heat flux on the wall), we introduce new variable

$$\tilde{u} = \frac{u}{u_m}, \quad R = \frac{r}{r_0}, \quad X = \frac{2}{Pe}\frac{x}{d}, \quad \theta = \frac{T - T_0}{\left(\frac{qd}{\lambda}\right)} \tag{13}$$

where $Pe = \frac{\bar{u}d}{\alpha}$, $\tilde{u} = (1 - R^2)$, $d = 2r_0$, u_m and $\bar{u} = u_m/2$ are the axial and average velocities, respectively, T_0 is the fluid temperature at the entrance of the heating section, α is the thermal diffusivity.

The dimensionless form of Eq. (12) is

$$\tilde{u}\frac{\partial \theta}{\partial X} = \frac{1}{R}\frac{\partial}{\partial R}\left(R\frac{\partial \theta}{\partial R}\right) + \frac{1}{Pe^2}\frac{\partial^2 \theta}{\partial X^2} \tag{14}$$

Transferring Eq. (14) to divergent form and integrating this equation through the micro-channel cross-section we obtain:

$$\frac{\partial}{\partial X}\left(\int_0^1 \tilde{u}\theta R\,dR\right) = \left(R\frac{\partial \theta}{\partial R}\right)\Big|_0^1 + \frac{1}{Pe^2}\frac{\partial^2}{\partial X^2}\left(\int_0^1 \theta R\,dR\right) \tag{15}$$

Assuming that the exit of the micro-channel is connected to an adiabatic section the boundary conditions are:

$$X = 0, \quad \theta = 0, \quad X > 0 \begin{cases} R = 0, & \dfrac{\partial \theta}{\partial R} = 0 \\ R = 1, & \dfrac{\partial \theta}{\partial R} = \dfrac{1}{2} \end{cases}, \quad X = X_*, \quad \frac{\partial \theta}{\partial X} = 0 \tag{16}$$

where X_* corresponds to the micro-channel exit.

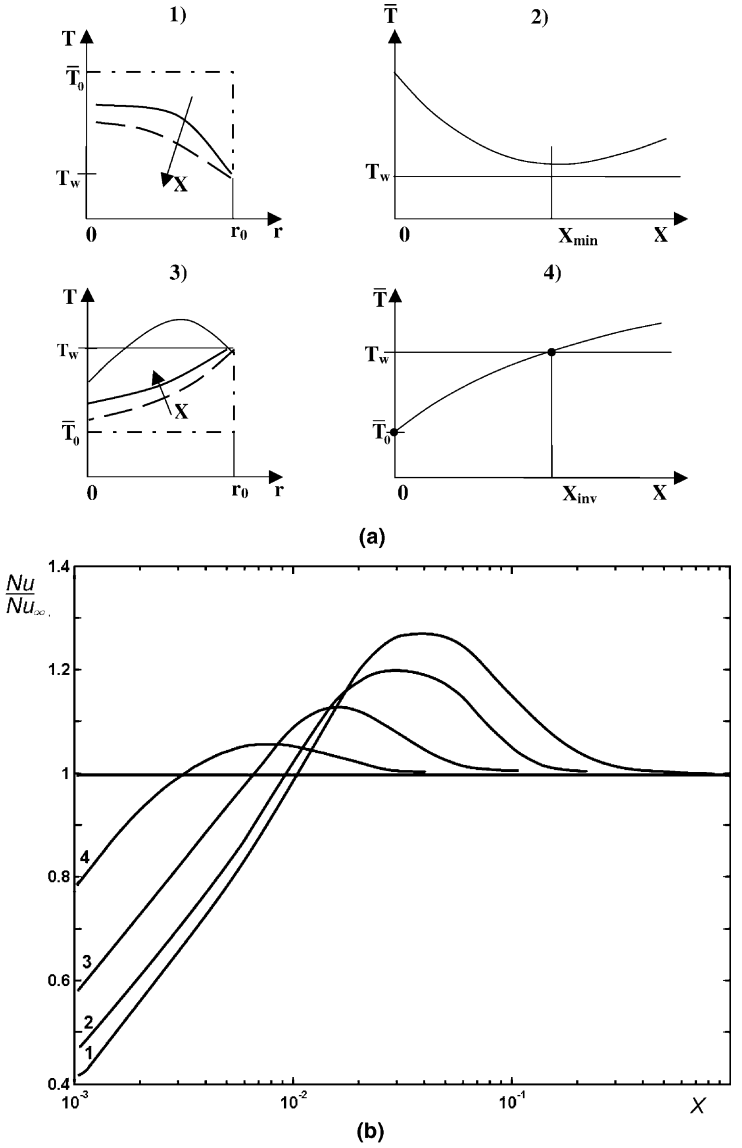

Fig. 8. Temperature distribution and heat transfer in micro-channels: (a) temperature distribution (1) and (2) $\overline{T}_0 > T_w$, (3) and (4) $\overline{T}_0 < T_w$ line –·–·– corresponds to temperature distribution at $X = 0$; arrow shows the direction of the increase of X. (b) Numerical calculations of the dependences $Nu(X)$; 1. $Pe = 1$, 2. $Pe = 2.5$, 3. $Pe = 10$, 4. $Pe = 45$, Petukhov [1, p. 200, Fig. 10.7].

Taking into account conditions (16) we obtain from (15):

$$\frac{\mathrm{d}}{\mathrm{d}X}\left(\int_0^1 \tilde{u}\theta R\,\mathrm{d}R\right) = \frac{1}{2} + \frac{1}{Pe^2}\frac{\mathrm{d}^2\bar{\theta}}{\mathrm{d}X^2} \tag{17}$$

where $\bar{\theta} = \int_0^1 \theta R\,\mathrm{d}R$ is the average temperature.

Assuming that θ is a weak function of R and $\theta \approx \bar{\theta}$ we can estimate:

$$\int_0^1 \tilde{u}\theta R\,\mathrm{d}R \approx \frac{\bar{\theta}}{4} \tag{18}$$

Then Eq. (17) is

$$\frac{\partial^2\bar{\theta}}{\partial X^2} - \frac{1}{4}Pe^2\frac{\partial\bar{\theta}}{\partial X} + \frac{1}{2}Pe^2 = 0 \tag{19}$$

The solution of the Eq. (19) is

$$\bar{\theta} = C_1 + C_2\exp\left(\frac{Pe^2}{4}X\right) + 2X \tag{20}$$

where C_1 and C_2 are constants.

Using the first and third conditions (16) we find:

$$C_1 = C_2, \quad C_2 = -\frac{2}{(Pe^2/4)} \exp\left(-\frac{Pe^2}{4} X_*\right) \tag{21}$$

The effect of axial conduction on heat transfer in the fluid in micro-channel can be characterized by dimensionless parameter

$$M = \frac{|F_{\text{cond}}|}{|F_{\text{conv}}|} \tag{22}$$

that expresses the correlation between heat fluxes due to conduction and convention. In Eq. (22) $F_{\text{conv}} = \rho \bar{u} c_p (T - T_0)$, $F_{\text{cond}} = \lambda \frac{\mathrm{d}T}{\mathrm{d}x}$. Substitution of the expression for variable $\bar{\theta}$ and $\frac{\partial \bar{\theta}}{\partial X}$ in relation (22) gives:

$$M = \frac{1}{4} \frac{1 - \exp(\chi - \chi_*)}{\chi - \exp(\chi - \chi_*) + \exp(-\chi_*)} \tag{23}$$

where $\chi = \frac{Pe^2 X}{4}$, $\chi_* = \frac{Pe^2 X_*}{4}$.

The limiting cases are:

(i) $\chi \ll 1, \chi_* \gg 1$

(ii) $\chi - \chi_* \ll 1 \begin{cases} \text{a.} & \chi_* \gg 1 \\ \text{b.} & \chi_* \ll 1 \end{cases}$

which corresponds to heat transfer at cooling inlet and heat transfer in the vicinity of the adiabatic outlet, respectively. In the first case we obtain the following evaluation of parameter M:

$$M = \frac{1}{4} \frac{1}{\chi} \gg 1 \tag{24}$$

It shows that close to the micro-channel inlet, heat losses to the cooling inlet due to axial conduction in the fluid are dominant. In the second case parameter M is

a. long micro-channel $M = \dfrac{\chi_* - \chi}{\chi_* - 1} \ll 1$ (25)

b. short micro-channel $M = \dfrac{\chi_* - \chi}{\chi_*} \ll 1$ (26)

In this region of flow parameter, M decreases when χ increases (i.e. growth of the Peclet number). Accordingly the Nusselt number decreases with growth of the Peclet number and approaches to its limiting value Nu_∞ that corresponding to $Pe \to \infty$.

The existence of heat transfer due to axial conduction in the fluid leads to increasing difference between wall-fluid temperature and decreasing value of the Nusselt number within the entrance section as compared to Nu_∞. These effects are illustrated in Fig. 8b. It is possible to estimate the critical value of the parameter M that subdivided the states at which the effect of axial conduction dominates ($M > M_{\text{cr}}$) or it is negligible ($M < M_{\text{cr}}$). According to the data of Petukhov [1], the critical value of parameter M is $M_{\text{cr}} \simeq 0.01$. In line with these results we obtain the following evaluation of the length where the effect of axial conduction in the fluid should be taken into consideration: $\frac{x}{r_0} Pe \leqslant 20$.

4.2. Axial conduction in the wall

This problem was considered by Petukhov [1]. The parameter used to characterize the effect of axial conduction is: $P = \left(1 - \frac{d_2^2}{d_1^2}\right) \frac{\lambda_2}{\lambda_1}$. The numerical calculations performed for $q = \text{const}$ and neglecting the thermal wall resistance in radial direction, showed that axial thermal conduction in the wall does not affect the Nusselt number, Nu_∞. Davis and Gill [64] considered the problem of axial conduction in the wall with reference to laminar flow between parallel plates with finite conductivity. It was found that Peclet number, ratio of thickness of the plates to their length, δ_2/L, as well as the ratio of parameter $\frac{\lambda_2}{L} / \frac{\lambda_1}{\delta_1}$ are an important dimensionless groups that determine the process of heat transfer.

The effect of axial conduction in the wall on the heat transfer in micro-channels was recently investigated by Maranzana et al. [24] and Tiselj et al. [59]. In the first study the thermal structure of laminar flow between parallel plates was investigated. In the second one, heat transfer characteristics of water flowing through triangular silicon micro-channel were analyzed. For physical interpretation the effects due to axial conduction in the wall Maranzana et al. [24] introduced "axial conduction number", M, defined as the ratio of conductive heat flux to convective one. Numerical calculations by Maranzana et al. [24] showed that the effect of axial conduction in the wall are significant when parameter $M > 10^{-2}$. According to Tiselj et al. [59] axial conduction in the wall affects significantly the longitudinal fluid and wall temperature distribution and longitudinal distribution of the normal and axial heat flux. We discuss these results in Section 5.

4.3. Combined axial conduction in the fluid and in the wall

The energy equations for the fluid and the solid wall are [1,65]:

$$\frac{\partial \tilde{u} \theta_1}{\partial X} = \frac{1}{R} \frac{\partial}{\partial R} \left(R \frac{\partial \theta_1}{\partial R} \right) + \frac{1}{Pe^2} \frac{\partial^2 \theta_1}{\partial X^2} \tag{27}$$

$$\frac{1}{R} \frac{\partial}{\partial R} \left(R \frac{\partial \theta_2}{\partial R} \right) + \frac{1}{Pe^2} \frac{\partial^2 \theta}{\partial X^2} = 0 \tag{28}$$

where $\theta_i = (T_i - T_0)/(\frac{q d_1}{\lambda_i})$, $i = 1, 2$ for the fluid and wall, respectively.

Integration of Eqs. (27), (28) through the cross-section of the micro-channel gives:

$$\frac{\partial}{\partial X}\left(\int_0^1 \tilde{u}\theta_1 R\,\mathrm{d}R\right)=\left(R\frac{\partial\theta_1}{\partial R}\right)\Big|_0^1+\frac{1}{Pe^2}\frac{\partial^2}{\partial X^2}\left(\int_0^1\theta_1 R\,\mathrm{d}R\right) \tag{29}$$

$$\left(R\frac{\partial\theta_2}{\partial R}\right)\Big|_1^{R_*}+\frac{1}{Pe^2}\frac{\partial^2}{\partial X^2}\left(\int_1^{R_*}\theta_2 R\,\mathrm{d}R\right)=0 \tag{30}$$

where

$$\left.\frac{\partial\theta_1}{\partial R}\right|_0=0,\quad \left(\frac{\partial\theta_1}{\partial R}=\frac{\partial\theta_2}{\partial R}\right)\Big|_{R=1}=0,\quad \left.\frac{\partial\theta_2}{\partial R}\right|_{R=R_*}=\frac{\lambda_1}{\lambda_2}\frac{1}{2} \tag{31}$$

The sum of Eqs. (29) and (30) is

$$\begin{aligned}\frac{\partial}{\partial X}&\left(\int_0^1\tilde{u}\theta_1 R\,\mathrm{d}R\right)\\&=\left(R\frac{\partial\theta_2}{\partial R}\right)\Big|_{R=R_*}+\frac{1}{Pe^2}\frac{\partial^2}{\partial X^2}\left(\int_0^1\theta_1 R\,\mathrm{d}R\right)\\&\quad+\frac{1}{Pe^2}\frac{\partial^2}{\partial X^2}\left(\int_1^{R_*}\theta_2 R\,\mathrm{d}R\right)\end{aligned} \tag{32}$$

Taking into account that

$$\bar{\theta}_1=\int_0^1\theta_1 R\,\mathrm{d}R,\quad \bar{\theta}_2=(R_*^2-1)^{-1}\int_1^{R_*}\theta_2 R\,\mathrm{d}R \tag{33}$$

we obtain:

$$\frac{\mathrm{d}}{\mathrm{d}X}\left(\int_0^1\tilde{u}\theta_1 R\,\mathrm{d}R\right)=\frac{\lambda_1}{\lambda_2}\frac{1}{2}+\frac{1}{Pe^2}\frac{\mathrm{d}^2\bar{\theta}_1}{\mathrm{d}X^2}+\frac{(R_*^2-1)}{Pe^2}\frac{\mathrm{d}^2\bar{\theta}_2}{\mathrm{d}X^2} \tag{34}$$

Assuming that $\frac{\mathrm{d}^2\bar{\theta}_1}{\mathrm{d}X^2}\approx\frac{\mathrm{d}^2\bar{\theta}_2}{\mathrm{d}X^2}$ the following equation for average fluid temperature was obtained:

$$\frac{\mathrm{d}^2\bar{\theta}_1}{\mathrm{d}X^2}-\frac{Pe^2}{4R_*^2}\frac{\mathrm{d}\bar{\theta}_1}{\mathrm{d}X^2}+\frac{1}{2}\lambda_{1,2}\frac{Pe^2}{R_*^2}=0 \tag{35}$$

The longitudinal fluid temperature distribution is

$$\bar{\theta}_1=C_1+C_2\exp\left(\frac{Pe^2}{4R_*^2}X\right)+2\frac{\lambda_1}{\lambda_2}X \tag{36}$$

where $C_1=-C_2$; $C_2=-\frac{2(\lambda_1/\lambda_2)}{(Pe^2/4R_*^2)}\exp\left(\frac{Pe^2X_*}{4R_*^2}\right)$ and the parameter M is

$$M=\frac{1}{4}\frac{1-\exp(\tilde{\chi}-\tilde{\chi}_*)}{(\lambda_1/\lambda_2)\tilde{\chi}-\exp(\tilde{\chi}-\tilde{\chi}_*)+\exp(-\tilde{\chi}_*)} \tag{37}$$

where $\tilde{\chi}=\frac{Pe^2X}{4R_*^2}$, $\tilde{\chi}_*=\frac{Pe^2X_*}{4R_*^2}$.

For the limiting cases $\tilde{\chi}\ll 1$ and $\tilde{\chi}_*\gg 1$ we obtain the following estimation:

$$M=\frac{1}{4\lambda_{1,2}}\frac{1}{\tilde{\chi}}=\frac{\Lambda}{4\chi} \tag{38}$$

where $\Lambda=\frac{\lambda_2}{\lambda_1}\left(\frac{r_2}{r_1}\right)^2$. For conditions corresponding to flow in micro-channels, the factor is $\Lambda\gg 1$. For example Λ equals 25 and 250 for water flows in micro-channels of $r_2/r_1=1.1$ made of stainless steel and silicon walls, respectively. That shows that conduction in the wall has significant effect on the heat transfer in micro-channels. It can be an important factor that leads to changing heat transfer coefficient.

5. The features of micro-channel heat sinks

5.1. Three-dimensional heat transfer in micro-channel heat sinks

The cooling systems fabricated from large number of rectangular [52,66,67] triangular [59] or circular [68] micro-channels were investigated both theoretically and experimentally. The micro-channel heat sinks are highly complicated systems with non-uniform distribution of thermal characteristics. The existence of non-uniform temperature field in the liquid and solid substrate leads to non-uniform distribution of heat fluxes in the streamwise and spanwise direction. Qu and Mudawar [52] carried out calculations at $Re=140$, 700, 1400 for heat sink that consists of a 1 cm^2 silicon wafer. The micro-channels had a width of 57 μm, and a depth of 180 μm, and were separated by a 43 μm wall. The major approximations introduced in the classical fin analysis method for micro-channel heat sinks operating in the laminar flow regime are summarized and assessed based on numerical results. The numerical results of this study revealed that classical fin method can only provide a qualitatively correct picture of the heat transport in a micro-channel heat sink.

Numerical results of heat transfer inside four 1 cm^2 heat sinks for number of channels 150 and 200 were presented by Toh et al. [66]. The calculation predicted the local thermal resistance very well. The micro-heat sink modeled in numerical investigation by Li et al. [67] consisted of a 10 mm long silicon substrate. The rectangular micro-channels had a width of 57 μm, and a depth of 180 μm. The heat transfer calculations were performed for Reynolds numbers 144, 77 and 42. The longitudinal heat conduction along the silicon wafer at different Reynolds number is different. In reality, because it is difficult to achieve an adiabatic boundary at the inlet and outlet of the heat sink as assumed in the numerical model, a significant portion of the heat is transferred to the inlet and outlet manifolds, especially for low fluid flow conditions. Thus, when evaluating the heat transfer in micro-heat sinks with low fluid flow rates, particular attention should be paid to the effects of heat conduction through the wafer.

Kroeker et al. [68] investigated thermal characteristics of heat sinks with circular micro-channels using

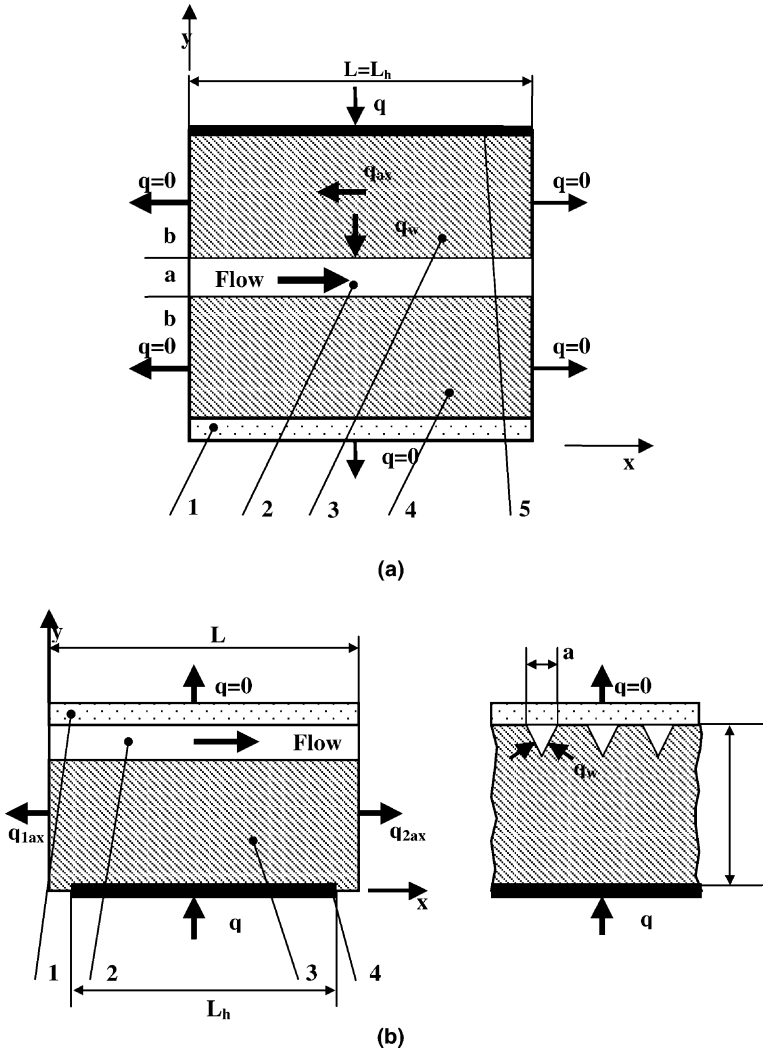

Fig. 9. Effect of axial conduction. Calculation models. (a) Channel between two parallel plates, Maranzana et al. [24]: 1—Cover plate, 2—micro-channel, 3—silicon block 1, 4—silicon block 0, 5—heater. (b) Calculation model of triangular micro-channels heat sink, Tiselj et al. [59]: 1—Cover plate, 2—micro-channel, 3—silicon wafer, 4—heater.

the continuum model based on the conventional Navier–Stokes equations and the energy conservation equation. Developing flow (both hydrodynamic and thermal) was assumed in the flow region and three-dimensional conjugate heat transfer was assumed in the solid region. At the inlet and at the exit of the solid (copper or silicon) adiabatic boundary conditions were imposed. The calculations of local Nusselt number performed at $Re = 500$ and $Re = 1000$ follow closely the classical solution reported by Shah and London [54] for forced convection in tubes with constant wall temperature.

One particular characteristic of conductive heat transfer in micro-channel heat sinks is the strong three dimensional character of the phenomenon. The lower the hydraulic diameter is, the more important the coupling between wall and bulk fluid temperatures becomes because the heat transfer coefficient reaches large values. Even though the thermal wall boundary conditions at the inlet and outlet of the solid wall are adiabatic, for small Reynolds numbers the heat flux can become strongly non-uniform: most of the flux is transferred to the fluid flow at the entrance of the micro-channel. Maranzana et al. [24] analyzed this type of problem and proposed the model of channel flow heat transfer between parallel plates. The geometry shown in Fig. 9a corresponds to a flow between parallel plates, the uniform heat flux is imposed on the upper face of block 1; the lower face of block 0 and the side faces of both

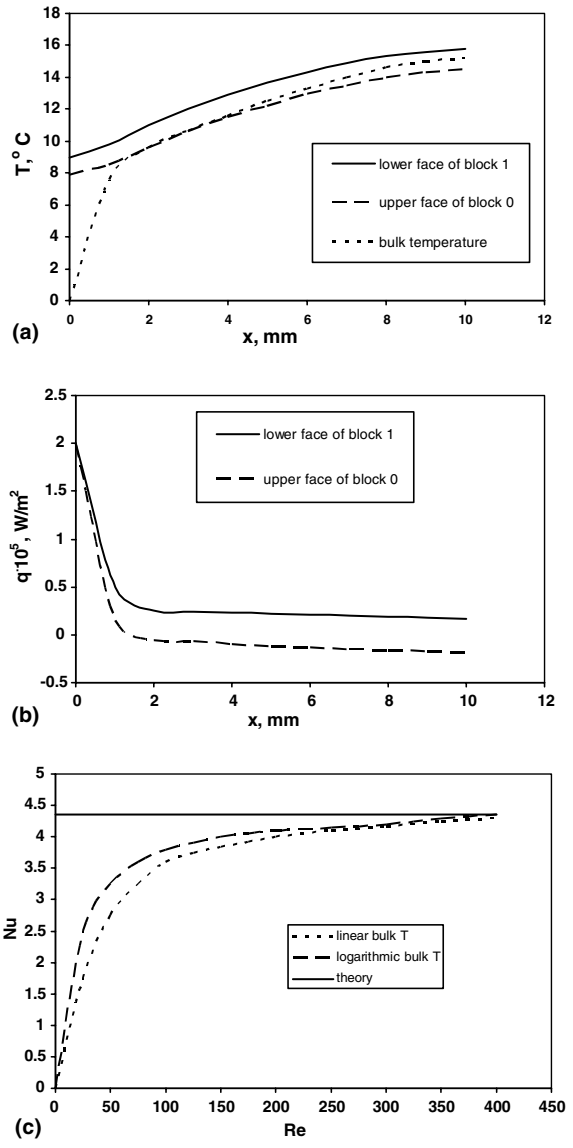

Fig. 10. Effect of axial conduction. Channel between two parallel plates. Numerical simulation. Maranzana et al. [24]: (a) interface temperature, (b) interface heat flux, (c) the Nusselt numbers.

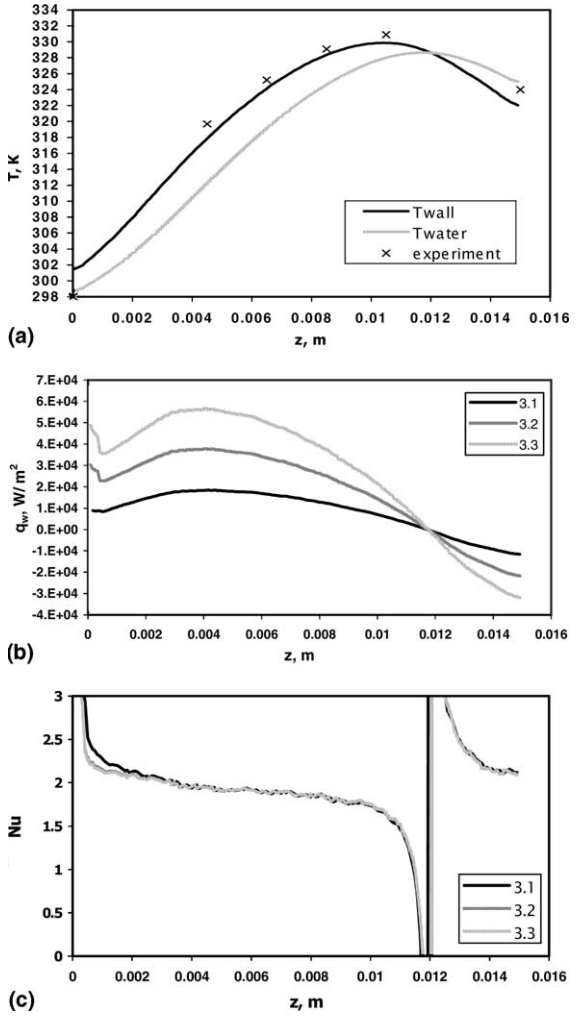

Fig. 11. Effect of axial conduction. Triangular micro-channels. $\dot{m} = 0.0356$ g/s. Tiselj et al. [59]. (a) Average water and silicon temperature distributions. $N = 8.424$ W. (b) Wall normal heat flux distribution in the silicon chip. 3–1 $N = 2.816$ W, 3–2 $N = 5.676$ W, 3–3 $N = 8.424$ W. (c) Axial distribution of the Nusselt number in the chip. 3–1 $N = 2.816$ W, 3–2 $N = 5.676$ W, 3–3 $N = 8.424$ W.

blocks are adiabatic. The two 10 mm long and 500 μm thick blocks are made of silicon, water flows in the 100 μm thick channel. Fig. 10a–c shows interface temperature, interface heat flux and the Nusselt number. The lower the Reynolds number is the larger the axial conduction effects become.

The numerical and experimental study of Tiselj et al. [59] was focused on effect of axial heat conduction through silicon wafer on heat transfer in the range of $Re = 3.2$–84. Compared to the case discussed by Maranzana et al. [24] the thermal wall boundary conditions at the inlet and outlet of the solid wall are not adiabatic. The heat sink was fabricated of a square-shape silicon substrate 15×15 mm^2, 530 μm thick. In the silicon substrate, 17 parallel micro-channels were etched. The cross-section of each channel was an isosceles triangle with a base of 310 μm, the length of the micro-channels was $L = 15$ mm, the heating length was $L_h = 10$ mm. The angles at the base were 55°, the hydraulic diameter was $D_h = 160$ μm. The experimental results were used for numerical calculation. The calculation model is presented in Fig. 9b.

The bulk water temperature and wall temperature on the inner heated wall of the triangular channel is shown in Fig. 11a. Both temperatures did not change linearly along the longitudinal direction. In fact, a linear temperature rise cannot be regarded as a good approximation for both temperatures. When axial heat flux is directed to both the inlet and the outlet manifolds the water and heated surface temperatures did not change monotonously. The longitudinal distributions of the silicon-fluid wall normal cross-section heat fluxes are presented in Fig. 11b. The heat fluxes are taken to be positive if they are directed from the solid to the fluid, and negative, otherwise. The direction and the magnitude of the negative heat flux depend on relation between the two thermal resistances: the first defines the heat transport from the wall through the boundary layer to the fluid core, and the second one quantifies the possibility of heat transport through silicon wafer. The importance of the second alternative pathway for the heat transfer can be truly appreciated only in three-dimensional conjugate heat transfer problem. The thermal wall boundary conditions have a dominant role in such a problem. Numerical predictions of the local Nusselt number variation in the streamwise direction are plotted in Fig. 11c. As indicated by Incropera and De Witt [69] the thermal entry length of a circular tube is

$$L_{\mathrm{th}} = 0.05Pe \cdot d \tag{39}$$

In the study [59] the thermal entry length was 0.13 and 3.3 mm for $Re = 3.2$ and 84, respectively.

5.2. Entrance effects

The entrance effects in a single channels were well studied [1–4,7,67]. We restrict our discussion to effect of the inlet and the outlet manifold on the flow and the temperature distributions between the parallel micro-channels. Hetsroni et al. [70], Klein et al. [71] observed an uneven liquid distribution in the parallel micro-channels. Depending on particular manifold design, the difference between the flow rate into some parallel micro-channels ranged up to about 20%. Furthermore, due to relative high thermal conductivity of the manifolds, fluid pre-warming occurred in the inlet manifold and additional warming occurred in the outlet manifold. The behavior of the Nusselt number depends, at least partly, on the entrance effects, which may be important in the laminar regime. The problem was also studied by Gamrat et al. [7]. Idealizing the flow rate as uniform can result in a significant error in prediction of temperature distribution of the heated electronic device. Lee et al. [55] showed that the entrance and boundary conditions imposed in the experiment need to be carefully matched in the predictive approaches. In his case numerical predictions based on a classical, continuum approach were in good agreement with the experimental data.

5.3. Characteristic parameters

Two definitions were considered by Qu and Mudawar [72] for heat flux to the heat sink. The first is an "effective" heat flux defined as the total electrical power input divided by the top area of the heat sink. The second definition is a mean heat flux averaged over the micro-channel heated inside area. We determined heat flux as the power calculated from the energy balance based on fluid temperature at the inlet and outlet manifolds, divided by the heated area of the micro-channel side walls [59]. Often special effects are proposed to explain unexpected experimental results, great care has to be paid for inversion of the temperature measurements. A common assumption often made [9–11] is to consider the wall heat flux to be uniform along the channels. However, according to Figs. 10b and 11b wall heat flux was far from uniform. As shown in Figs. 6c, 10a and 11a the bulk temperature of the fluid did not vary linearly [18]. This effect is especially important when the M number is large. For example, Maranzana et al. [24] utilized exact modeling of heat conduction in the wall. The corresponding simulated estimation of the convective heat transfer coefficient at $M = 0.32$ was equal to 25,905 $\mathrm{W/m^2\,K}$. By comparison the one-dimensional model, assuming that the bulk temperature is linear, yields a mean convective heat transfer coefficient of 6100 $\mathrm{W/m^2\,K}$. Axial conduction can be neglected as soon the M number gets lower than 0.01.

5.4. Effect of wall roughness

The roughness leads to increasing friction factor at the same Reynolds number. The existence of roughness leads also to decreasing the value of the critical Reynolds number, at which occurs transition from laminar to turbulent flow. We suggested a following estimate of the relative roughness, corresponding to the hydrodynamic boundary that subdivides the flow in smooth and rough channels [60] $k_s/r < 5/1.41Re^{0.5}$, where k_s if the height of roughness, r is the channel hydraulic radius, Re is the Reynolds number. For $Re \sim 2000$, the relative roughness that corresponds to the boundary between the smooth and roughness channels is about 0.08. Turner et al. [73] concluded that micro-channel surfaces with relative surface roughness of 0.06 did not cause any statistical change in the friction factor for laminar flow. The effect of surface roughness on heat transfer depends on the Prandtl number. Kandlikar et al. [50] reported that for 1067 μm diameter tube, the effect of relative roughness about 0.003 on heat transfer in water flow was insignificant. For 620 μm this relative roughness increases the

heat transfer. New experiments should be performed to clarify the effect of wall roughness on heat transfer.

5.5. Interfacial effects

Turner et al. [74] reported that for the Knudsen number $Kn < 0.04$ (ratio of mean free path to channel hydraulic diameter) the continuum based equations can be used for flow in micro-channels. Because the micro-devices have a large surface to volume ratio, factors related to surface effects have more impact to the flow at small scales. Among these are the surface electrostatic charges. If the liquid contains even very small amounts of ions, the electrostatic charges on the solid surface will attract the counter ions in the fluid to establish an electrical field. The arrangement of the electrostatic charges on the solid surface and the balancing charges in the liquid is called the electrical double layer (EDL). Mala et al. [75], Yang and Li [76] Ren et al. [77] reported numerical and experimental results for the EDL effect with different liquids. They found that the EDL effect led to higher friction coefficient for pure water and dilute solutions. No results for heat transfer were presented.

5.6. Effect of measurement accuracy

In experiments of flow and heat transfer in micro-channels, some parameters, such as the Reynolds number, heat transfer coefficient, the Nusselt number are difficult to obtain with high accuracy. The channel hydraulic diameter measurement error may play very important part in the uncertainty of the friction factor [60]. The analysis carried out by Hetsroni et al. [78] for micro-tube reveals the following values of standard uncertainties: infrared measurements- systematic error 0.1 K, random error 0.2 K; thermocouples-systematic error 0.1 K, random error 0.15 K; temperature acquisition system- systematic error 0.1 K, random error 0.16 K. The 95% confidence uncertainty of the heat transfer coefficient was 13.2%. The uncertainty must be taken into account by presentation of experimental data and by comparison between experiments and theoretical predictions.

6. Conclusions

Heat transfer in micro-channels occurs under conditions of strong superposition of hydrodynamic and thermal effects, determining the main characteristics of this process. The experimental study of the heat transfer is a complex problem because of the small sizes of such channels. It makes difficult direct diagnostic of temperature field in fluid flow and in solid wall. The certain information on mechanisms of this phenomenon can be obtained by analysis of the data of experiments, in particular, by comparison of data of measurements with predictions that are based on several models of heat transfer in circular, rectangular and trapezoidal micro-channels. This approach makes it possible to estimate the applicability of the conventional theory, and the correctness of several hypotheses related to the mechanism of heat transfer. It is possible to reveal the effects of: the Reynolds number, axial conduction, energy dissipation, heat losses to the environment, etc. on the heat transfer.

The theoretical models used for this purpose can be conditionally subdivided in two groups depending on the degree of correctness of the assumptions. The first of these groups includes the simplest one-dimensional models assuming uniform heat flux, constant heat transfer coefficient, etc. The comparison of these models with experiment shows significant discrepancy between the measurements and the theoretical predictions. Using some "new effects", which are not described by conventional Navier–Stokes and energy equations, the simple models may explain experimental results. The second group is based on numerical solution of full Navier–Stokes and energy equations, which account for the real geometry of the micro-channel, axial conduction in the fluid and wall, energy dissipation, non adiabatic thermal boundary condition at the inlet and outlet of the heat sink, dependence of physical properties of fluid on temperature, etc. These models demonstrate a fairly well correlation with data of available experimental data. As a rule, the numerical calculations using simple models were performed for the following hydraulic boundary conditions:

(1) a uniform velocity profile was set at the channel inlet
(2) the flow was assumed to be fully developed at the test section
(3) all the fluid properties are constant.

The thermal boundary conditions were set as follows:

(1) constant heat flux at the walls
(2) adiabatic conditions at the inlet and outlet.

These boundary conditions are not in agreement with experiments for which the "new effects" were assumed. As a result, the authors concluded that conventional Navier–Stokes and energy equations are not valid and only "new effects" can explain the experimental data. The numerical solutions based on Navier–Stokes and energy equations and taken proper account of boundary conditions demonstrate a fairly good agreement with available experimental data. The results can be generalized as follows:

1. The effect of energy dissipation on heat transfer in micro-channels is negligible under typical flow conditions.

2. Axial conduction in the fluid and wall affects significantly the heat transfer in micro-channels. At laminar flow two heat transfer regimes may be considered. The first of them takes place at $Re > 150$ and the axial conduction number is less than $M = 0.01$. Under this condition the heat transferred through the solid substrate may be neglected and adiabatic boundary conditions may be imposed at the inlet and at the outlet manifolds to solve conjugated three-dimensional heat transfer problem. The second one occurs at $Re < 150$, $M > 0.01$. In this case the heat transferred through the solid substrate should be taken into account.
3. The following considerations must be taken into account in the evaluation of any experimental results:
   (i) The experimental results based on the measurements of the fluid temperature only at the inlet and the outlet manifolds of the heat sink may lead to incorrect values of the Nusselt number.
   (ii) Since it is difficult to measure the local heat flux at the inner channel wall, the definition of the heat transfer coefficient is very important and will strongly influence the heat transfer coefficient.
4. Accurate estimation of the heat transferred through the solid substrate in experiments should be obtained from energy balance that include electric power (simulating the electronic components on the top or bottom wall of the heat sink), convective heat to the fluid (based on fluid mass flow rate and bulk fluid temperature measured at the inlet and outlet manifolds) and heat losses.
5. The experimental heat transfer coefficient calculated numerically using exact model with regard to the heat transferred through the solid substrate represents the correct variation of the Nusselt number with respect to the Reynolds number.
6. The thermal entry length should be considered by comparison between experimental and numerical results.

Acknowledgement

This research was supported by the Fund for Promotion of Research at the Technion. A. Mosayk is supported by a joint grant from the Center for Absorbtion in Science of the Ministry of Immigrant Absorbtion and the Committee for Planning and Budgeting of the Council for Higher Education under the framework of the KAMEA PROGRAM.

References

[1] B.S. Petukhov Heat transfer and drag of laminar flow of liquid in pipes. Energy, Moscow, 1967.
[2] W.M. Kays, M.E. Crawford, Convective Heat and Mass Transfer, McGraw-Hill, New York, 1993.
[3] H.D. Baehr, K. Stephan, Heat and Mass Transfer, Springer, 1998.
[4] H. Shlichting, Boundary Layer Theory, eighth ed., Springer, Berlin, 2000.
[5] C.M. Ho, Y.-C. Tai, Micro-electronic mechanic systems (MEMS) and fluid flows, Ann. Rev. Fluid Mech. 30 (1998) 5–33.
[6] M. Gad-el-Hak, The fluid mechanics of micro-devices. The Freeman Scholar Lecture, J. Fluid Eng. 121 (1999) 5–33.
[7] G. Gamart, M. Favre-Marinet, D. Asendrych, Conduction and entrance effects on laminar liquid flow and heat transfer in rectangular micro-channels, Int. J. Heat Mass Transfer 48 (2005) 2943–2954.
[8] S. Reynaud, F. Debray, J.-P. Frans, T. Maitre, Hydrodynamics and heat transfer in two-dimensional mini-channels, Int. J. Heat Mass Transfer 48 (2005) 3197–3211.
[9] B.X. Wang, X.F. Peng, Experimental investigation on liquid forced- convection heat transfer through micro-channels, Int. J. Heat Mass Transfer 37 (1) (1994) 73–82.
[10] X.F. Peng, G.P. Peterson, The effect of thermofluid and geometric parameters on convection of liquid through rectangular micro-channels, Int. J. Heat Mass Transfer 38 (1995) 755–758.
[11] X.F. Peng, G.P. Peterson, Convective heat transfer and flow friction for water flow in micro-channel structures, Int. J. Heat Mass Transfer 39 (1996) 2599–2608.
[12] X.F. Peng, B.X. Wang, G.P. Peterson, N.B. Ma, Experimental investigation of heat transfer in flat plates with rectangular micro-channels, Int. J. Heat Mass Transfer 38 (1995) 127–137.
[13] H.B. Ma, G.P. Peterson, Laminar friction factor in microscale ducts of irregular cross-section, Microscale Thermophys. Eng. 1 (1997) 253–265.
[14] G.M. Mala, D. Li, J.D. Dale, Heat transfer and fluid flow in micro-channels, Int. J. Heat Mass Transfer 40 (1997) 3079–3088.
[15] G.M. Mala, D. Li, Flow characteristics of water in microtubes, Int. J. Heat Fluid Flow 20 (1999) 142–148.
[16] W. Qu, G.M. Mala, D. Li, Heat transfer for water flow in trapezoidal silicon micro-channels, Int. J. Heat Mass Transfer 43 (2000) 3925–3936.
[17] W. Qu, I. Mudawar, Experimental and numerical study of pressure drop and heat transfer in a single-phase micro-channel heat sink, Int. J. Heat Mass Transfer 45 (2002) 2549–2565.
[18] P. Gao, S. Le Person, M. Favre-Marinet, Scale effects on hydrodynamics and heat transfer in two-dimensional mini and micro-channels, Int. J. Thermal Sci. 41 (2002) 1017–1027.
[19] C.Y. Zhao, T.J. Lu, Analysis of micro-channels for electronic cooling, Int. L. Heat Mass Transfer 45 (2002) 4857–4869.
[20] H.Y. Wu, P. Cheng, An experimental study of convective heat transfer in silicon micro-channels with different surface conditions, Int. J. Heat Mass Transfer 46 (2003) 2547–2556.
[21] B. Weigand, D. Lauffer, The extended Graetz problem with piecewise constant wall temperature for pipe and

channel flows, Int. J. Heat Mass Transfer 47 (2004) 5303–5312.
[22] P. van Male, M.H.J.M. de Croon, R.M. Tiggelaar, A. van den Derg, J.C. Schouten, Heat and mass transfer in a square micro-channel with asymmetric heating, Int. J. Heat Mass Transfer 47 (2004) 87–99.
[23] D. Lelea, S. Nishio, K. Takano, The experimental research on micro-tube heat transfer and fluid flow of distilled water, Int. J. Heat Mass Transfer 47 (2004) 2817–2830.
[24] G. Maranzana, I. Perry, D. Maillet, Mini- and micro-channels: influence of axial conduction in the walls, Int. J. Heat Mass Transfer 47 (2004) 3993–4004.
[25] C.P. Tso, S.P. Mahulikar, The use of the Brinkman number for single phase forced convective heat transfer in micro-channels, Int. J. Heat Mass Transfer 41 (1998) 1759–1769.
[26] C.P. Tso, S.P. Mahulikar, The role of the Brinkman number in analyzing flow transitions in micro-channels, Int. J. Heat Mass Transfer 42 (1999) 1813–1833.
[27] C.P. Tso, S.P. Mahulikar, Experimental verification of the role of the Brinkman number in micro-channels using local parameters, Int. J. Heat Mass Transfer 43 (2000) 1837–1849.
[28] G. Tunc, Y. Bayazitoglu, Heat transfer in micro-tubes with viscous dissipation, Int. J. Heat Mass Transfer 44 (2001) 2395–2403.
[29] J. Koo, C. Kleinstreuer, Viscous dissipation effects in micro-tubes and micro-channels, Int. J. Heat Mass Transfer 47 (2004) 3159–3169.
[30] D.K. Bailey, T.A. Ameel, R.O. Warrington Jr., T.I. Savoie, Single phase forced convection heat transfer in micro-geometries—A Review IEEC Papers No ES-369, ASME 1995, pp. 301–310.
[31] C.B. Sobhan, S.V. Garimella, A comparative analysis of studies on heat transfer and fluid flow in micro-channels, Microscale Thermophys. Eng. 5 (2001) 293–311.
[32] Z.-Y. Gua, Z.-X. Li, Size effect on micro-scale single-phase flow and heat transfer, Int. J. Heat Mass Transfer 46 (2003) 149–159.
[33] S. Kandlikar, W. Grande, Evolution of micro-channel flow passages-thermohydraulic performance and fabrication technology, in: Proceedings of IMEECE 2002, ASME International Mechanical Engineering Congress and Exposition, November 2002, New-Orleans, Louisiana, pp. 1–13.
[34] G.P. Celeta, M. Como, G. Zummo, Thermal-hydraulic characteristics of single-phase flow in capillary pipes, Exp. Thermal Fluid Sci. 28 (2004) 87–95.
[35] I. Hassan, P. Phuttavong, M. Abdelgawad, Micro-channel heat sinks: an overview of the state of the art, Microscale Thermophys. Eng. 8 (2004) 183–204.
[36] G.L. Morini, Single-phase convective heat transfer in micro-channels: overview of experimental results, Int. J. Thermal Sci. 43 (2004) 631–651.
[37] S.V. Garimella, C.B. Sobhan, Transport in micro-channels-a critical review, Ann. Rev. Heat Transfer 13 (2003) 1–50, Chapter I.
[38] M. Gad-el-Hak, Comments on "critical view on new results in micro-fluid mechanics, Int. J. Heat Mass Transfer 46 (2003) 3941–3945.
[39] H. Herwig, Flow and heat transfer in micro-systems, In: Everything Different or Just Smaller. ZAMM 0 (2000) 1–10.
[40] H. Herwig, O. Hausner, Critical view on "new results in micro-fluid mechanics: an example, Int. J. Heat Mass Transfer 46 (2003) 935–937.
[41] G. Hetsroni, M. Gurevich, A. Mosyak, R. Rozenblit, Drag reduction and heat transfer of surfactants flowing in a capillary tube, Int. J. Heat Mass Transfer 47 (2004) 3797–3809.
[42] E. Eckert, W. Weise, Die Temperatur unbeheizter Korper in einem Gasstrom hoher Geschwindigkeit, Forsch. Ing.-Wes. 12 (1941) 40–50.
[43] T.M. Adams, S.I. Abdel-Khalik, S.M. Jeter, Z.H. Qureshi, An experimental investigation of single-phase forced convection in micro-channels, Int. J. Heat Mass Transfer 41 (1998) 851–857.
[44] V. Gnielinski, New equations for heat and mass transfer in turbulent pipe and channel flow, Int. Chem. Eng. 16 (1976) 359–368.
[45] W. Owhaib, B. Palm, Experimental investigation of single-phase convective heat transfer in circular micro-channels, Exp. Thermal Fluid Sci. 28 (2004) 105–110.
[46] F.W. Dittus, L.M.K. Boelter, Heat transfer in automobile radiators of tubular type, Univ. California, Berkley, Publ. Eng. 2 (13), 1930, pp. 443–461.
[47] B. Petukhov, V. Kurgano, A. Gladuntsov, Heat transfer in turbulent pipe flow of gases with variable properties, Heat Transfer Sov. Res. 5 (1973) 109–116.
[48] P.Y. Wu, W.A. Little, Measuring of the heat transfer characteristics of gas flow in fine channel heat exchangers for micro-miniature refrigerators, Cryogenics 24 (1984) 415–420.
[49] S.B. Choi, R.F. Barron, R.Q. Warrington, Fluid flow and heat transfer in micro-tubes, in: D. Choi et al. (Eds.), Micro-Mechanical Sensors, Actuators and Systems, ASME DSC, vol. 32, 1991, pp. 121–128.
[50] S.G. Kandlikar, S. Joshi, S. Tian, Effect of surface roughness on heat transfer and fluid flow characteristics at low Reynolds numbers in small diameter tubes, Heat Transfer Eng. 24 (#3) (2003) 4–16.
[51] T.M. Harms, M.J. Kazmierzak, F.M. Gerner, Developing convective heat transfer in deep rectangular micro-channels, Heat and Fluid Flow, Int. J. Heat Fluid Flow 20 (1999) 149–157.
[52] W. Qu, I. Mudawar, Analysis of three-dimensional heat transfer in micro-channel heat sinks, Int. J. Heat Mass Transfer 45 (2002) 3973–3985.
[53] G.R. Warrier, V.K. Dhir, L.A. Momoda, Heat transfer and pressure drop in narrow rectangular channels, Exp. Thermal Fluid Sci. 26 (2002) 53–64.
[54] R.K. Shah, A.L. London, Laminar Flow Forced Convection in Ducts, Academic Press, New York, 1978, S.V.
[55] P.S. Lee, S.V. Garimella, D. Liu, Investigation of heat transfer in rectangular micro-channels, Int. J. Heat Mass Transfer 48 (2005) 1688–1704.
[56] J. Gruntfest, J.P. Young, N.L. Johnson, Temperatures generated by the flow of liquids in pipers, J. Appl. Phys. 35 (1964) 18–23.

[57] S.A. Bastanjian, A.G. Merzhanov, S.I. Xudiaev, On hydrodynamic thermal explosion, Sov. Phys. Docl. 163 (1965) 133–136.
[58] Ya.B. Zel'dovich, G.I. Barenblatt, V.B. Librovich, G.M. Maxhviladse, Mathematical Theory of Combustion and Explosion, Plenum, New York, 1985.
[59] I. Tiselj, G. Hetsroni, B. Mavko, A. Mosyak, E. Pogrebhyak, Z. Segal, Effect of axial conduction on the heat transfer in micro-channels, Int. J. Heat Mass Transfer 47 (2004) 2551–2565.
[60] G. Hetsroni, A. Mosyak, E. Pogrebnyak, L.P. Yarin, Fluid flow in micro-channels, Int. J. Heat Mass Transfer 48 (2005) 1982–1998.
[61] D.K. Hennecke, Heat transfer by Hagen-Poiseuille flow in the thermal development region with axial conduction, Wazme-Stoffubertz 1 (1968) 177–184.
[62] T.V. Nguyen, Laminar Heat transfer for thermal developing flow in ducts, Int. J. Heat Mass Transfer 35 (1992) 1733–1741.
[63] N.T. Nguyen, D. Bochnia, R. Kiehnscherrf, W. Dozel, Investigation of forced convection in micro-fluid systems, Sensors Actuators, A 55 (1996) 49–55.
[64] E.J. Davis, W.N. Gill, the effect of axial conduction in the wall on heat transfer with laminar flow, Int. J. Heat Mass Transfer 23 (1970) 459–470.
[65] L.I. Sedov, Similarity and Dimensional Methods in Mechanics, tenth ed., CRC Press, Boca Roton, Fla, 1993.
[66] K.C. Toh, X.Y. Chen, J.C. Chai, numerical computation of fluid flow and heat transfer in micro-channels, Int. J. Heat Mass Transfer 45 (2002) 5133–5141.
[67] J. Li, G.P. Peterson, P. Cheng, Three-dimensional analysis of heat transfer in a micro-heat sink with single phase flow, Int. J. Heat Mass Transfer 47 (2004) 4215–4231.
[68] C.J. Kroeker, H.M. Soliman, S.J. Ormiston, Three-dimensional thermal analysis of heat sinks with circular cooling micro-channels, Int. J. Heat Mass Transfer 47 (2004) 4733–4744.
[69] F.P. Incropera, D.P. De Witt, Fundamentals of Heat and Mass Transfer, fourth ed., Wiley, New York, 1996.
[70] G. Hetsroni, A. Mosyak, Z. Segal, Nonuniform temperature distribution in electronic devices cooled by flow in parallel micro-channels, IEEE Trans. Components Packag. Technol. 24 (#1) (2001) 16–23.
[71] D. Klein, G. Hetsroni, A. Mosyak, Heat transfer characteristics of water and APG surfactant solution in a micro-channel heat sink, Int. J. Multiphase Flow 31 (2005) 393–415.
[72] W. Qu, I. Mudawar, Measurement and correlation of critical heat flux in two-phase micro-channel heat sinks, Int. J. Heat Mass Transfer 47 (2004) 2045–2059.
[73] S.E. Turner, H. Sun, M. Faghri, O.J. Gregory, Effect of surface roughness on gaseous flow through micro-channels, ASME-Publications-HTD 366 (#2) (2000) 291–298.
[74] S.E. Turner, H. Sun, M. Faghri, O.J. Gregory, Local pressure measurement of gaseous flow through micro-channels, ASME-Publications-HTD 364 (#3) (1999) 71–80.
[75] G.M. Mala, D. Li, C. Werner, et al., Flow characteristics of water through a micro-channel between two parallel plates with electro kinetic effects, Int. J. Heat Fluid Flow 18 (1997) 491–496.
[76] C. Yang, D. Li, Analysis of electro kinetic effects on the liquid flow in micro-channels, Coll. Surf. A; Physicochem. Eng. Aspects 143 (1998) 339–353.
[77] L. Ren, W. Qu, D. Li, Interfacial electro kinetic effects on liquid flow in micro-channels, Int. J. Heat Mass Transfer 44 (2001) 3125–3134.
[78] G. Hetsroni, M. Gurevich, A. Mosyak, R. Rozenblit, Surface temperature measurement of a heated capillary tube by means of an infrared technique, Meas. Sci. Technol. 14 (2003) 807–814.